

Rapid Solidification

Cooling of liquid metals at rates higher than 1000°K/s

(compared with equilibrium cooling $\sim 10^{\circ}\text{K/h}$)

Melt lacks long range structural order, atomic positions fluctuate due to vibrations and diffusive motion
What if we freeze (“quench”) this state and avoid crystallization?

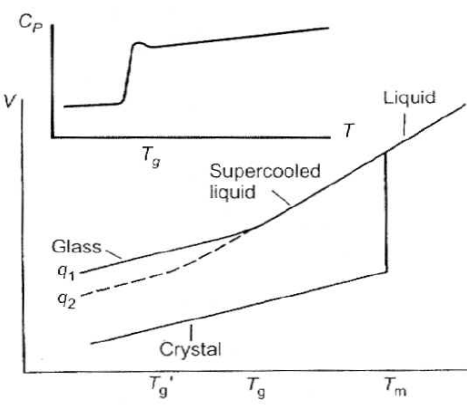
- Nonequilibrium phases if:
solidification velocity (growth rate) $v_{sl} > \text{diffusive speed } v_d = D/d_a$
- Microstructures nanocrystalline or amorphous
- Important for metallic glasses, Al-Ti-Mg alloys, shape memory alloys...

By avoiding crystallization, melt is supercooled below T_m very fast, **we avoid first order transition**

$$\Delta S = -\left(\frac{\partial G}{\partial T}\right)_P = \Delta V = \left(\frac{\partial G}{\partial P}\right)_T = 0$$

Glass transition from melt is a second order phase transition since there is a second order derivative change in G :

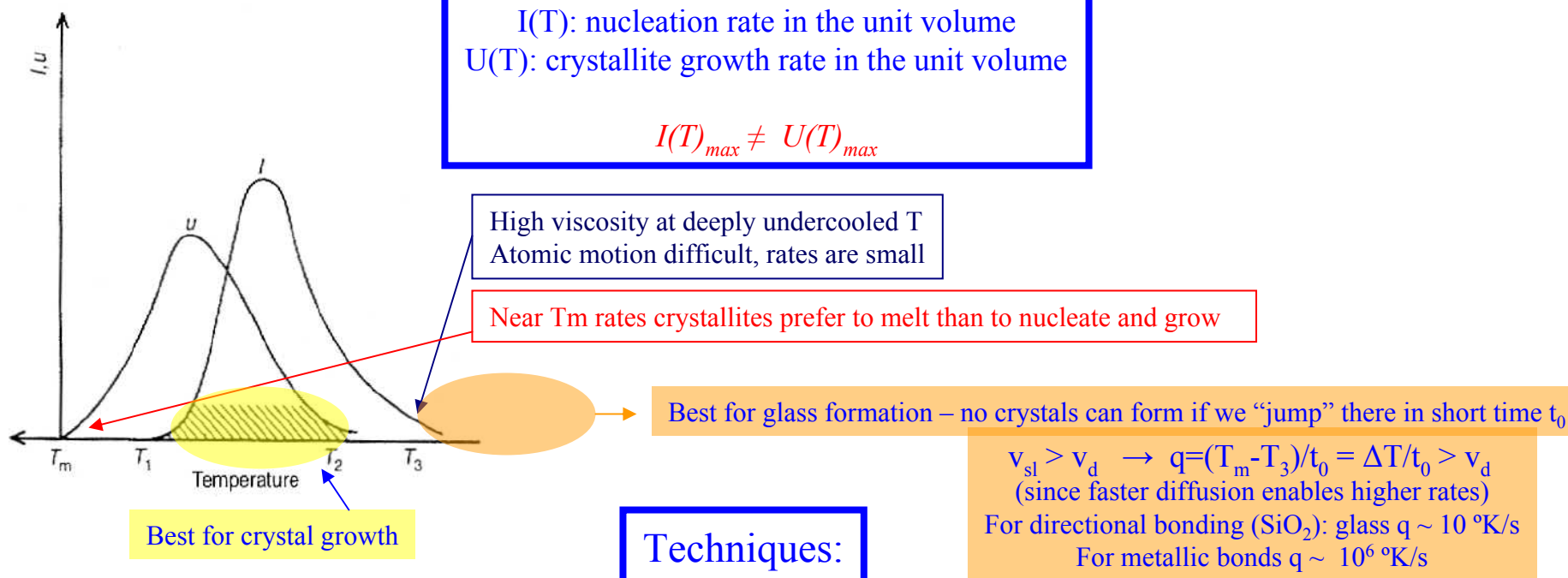
$$C_p = \left(\frac{\partial H}{\partial T}\right)_P = T\left(\frac{\partial S}{\partial T}\right)_P = -T\left(\frac{\partial^2 G}{\partial T^2}\right)_P$$



Influence of kinetics: melt supercooled with slower quenching rate q_2 has lower value of T_g

Looking from liquid side, there is increase in viscosity η of the melt ($\tau = \eta \partial v / \partial y$) until material behaves as a solid – but without crystallization.

Rapid Solidification



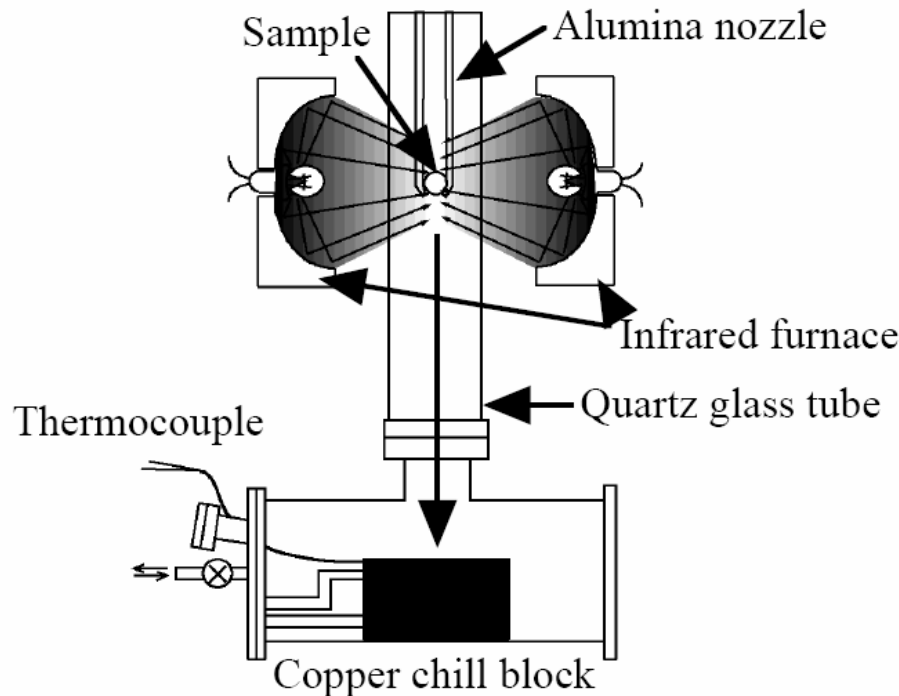
- *Splat cooling*: molten metal dropped onto substrate with high thermal conductivity held at room T or below
- *Melt spinning*: molten metal sprayed on rotating cold surface
- *Plasma spraying*: metal powder introduced into high T plasma or flame and sprayed on the substrate
- *Surface melting*: e-beam, laser beam..melts surface of a metal which resolidifies when the source of heat is removed.
- *Atomization* – stream of molten metal deposits on the cold surface with high velocity of solid – liquid interface avoiding nucleation of equilibrium solid phase.

Splat Cooling Example

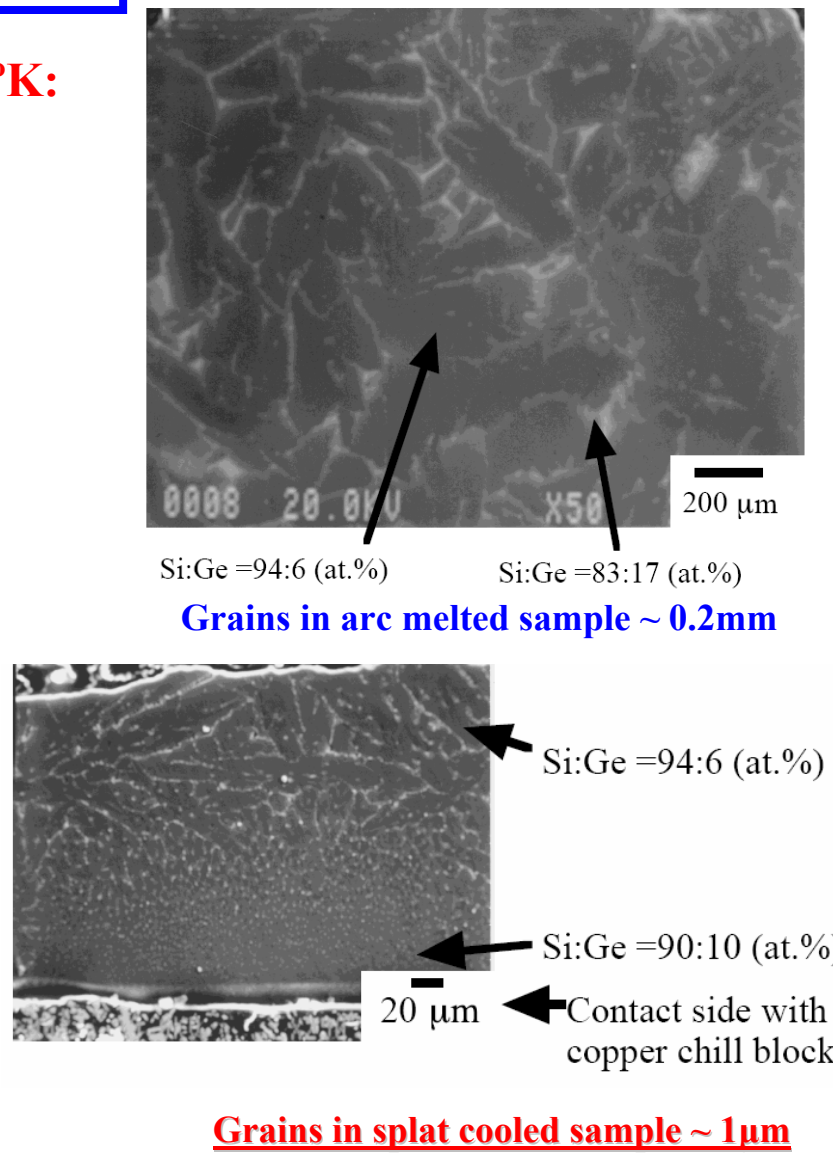
Jpn. J. App. Phys. 41, 749 (2002)

**Motivation: thermoelectric applications 900-1200°K:
decrease phonon scattering at grain boundaries**

(b) Splat solidification equipment

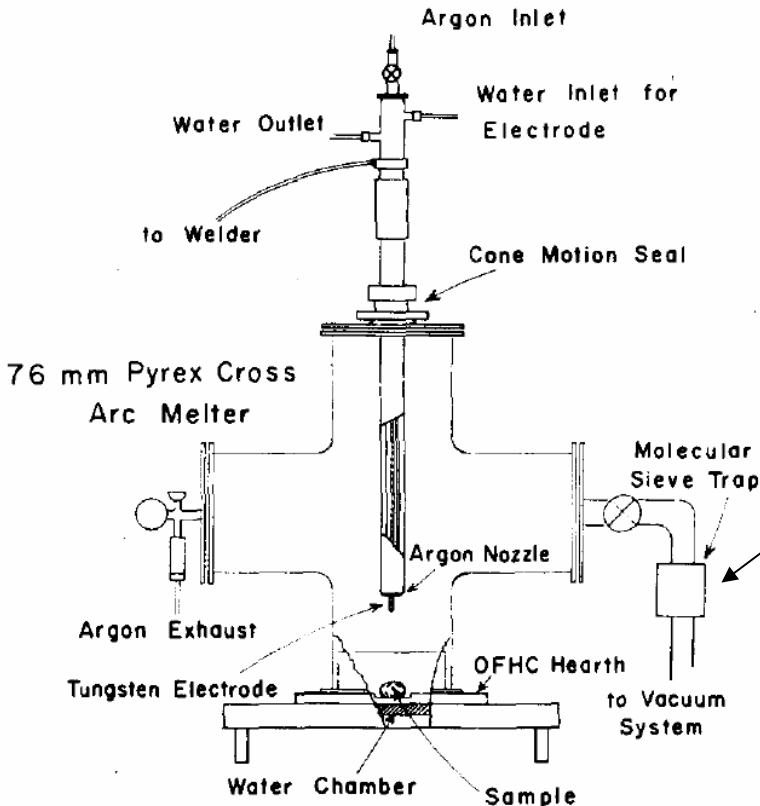


Splat cooling of melt obtained in
microgravity $10^{-4} g$
(more uniformity, less segregation)
Cooling rates $5000 K/s$



Arc Melting Furnace

Widespread in industry (~100 ton steel production) and laboratory (~ mg research samples)
Electric arc melts materials by passing current and by radiation heating
Often starting point in intermetallic flux growth



- Alternative to resistance or inductance heating
- Creating of alloys, powder melting
- Operating temperatures over 2000°C
- Top or bottom loading
- Cu stinger with W electrode
- Copper hearth
- Water cooling of electrode and hearth
- Vacuum pump
- Trap for hydrocarbons or oil free pump
- Inert gas system with relief valve
- Materials with low vapor pressure
- DC welding power supply ~40-300A
- Can be used for metal crucible sealing: Ta, Mo, W, Pt
- Sample space can be 360° visible
- Usual vacuum ~ 10^{-2} mbar
- Weight loss ~ 1% by weight

Arc Melting Furnace



CEA Grenoble (courtesy of Gerard Lapertot)



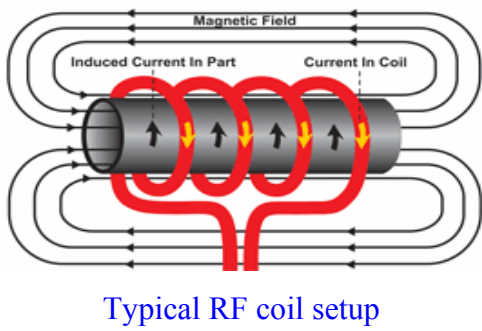
Petrovic lab at BNL

Bulk Synthesis in CMMP

Induction Heating

Heat induced in material by circulating electric currents as opposed to external application
No contact with flame, heater, coil itself is not hot, can reduce contamination

AC current applied to the coil , alternating magnetic field created:



$$B = B_0 e^{i\omega t}$$

Faraday law - *Emf* and circulating eddy currents are induced:

$$\varepsilon = -N \frac{\partial \Phi}{\partial t} = -N \frac{\partial}{\partial t} \int_S \vec{B} d\vec{S}$$

- Good for *thin* conductive materials (metals) – think of *skin effect* in conductors:

$$\vec{B}_{\text{int}}(z, t) = B_0(0) e^{-\frac{z}{\delta}} \cos\left(\omega t - \frac{z}{\delta}\right) \vec{e}_x$$
$$\delta = \frac{1}{\sqrt{\pi \mu \sigma}}$$

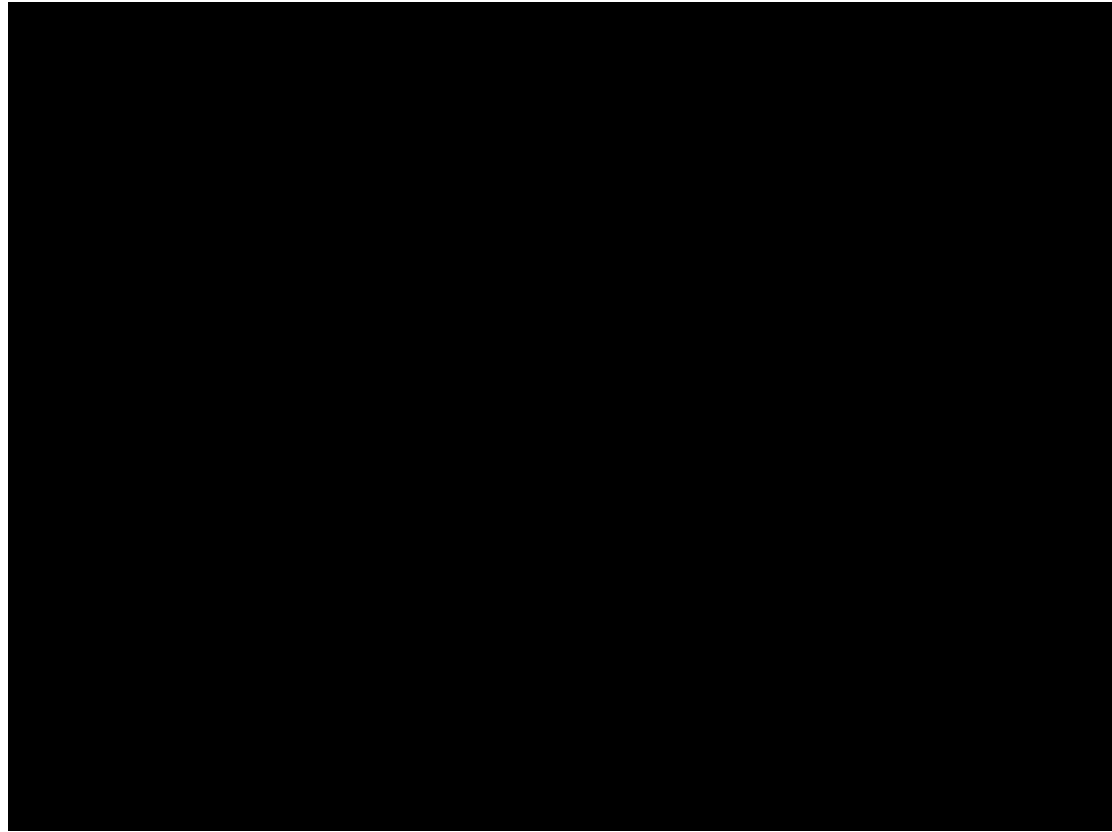
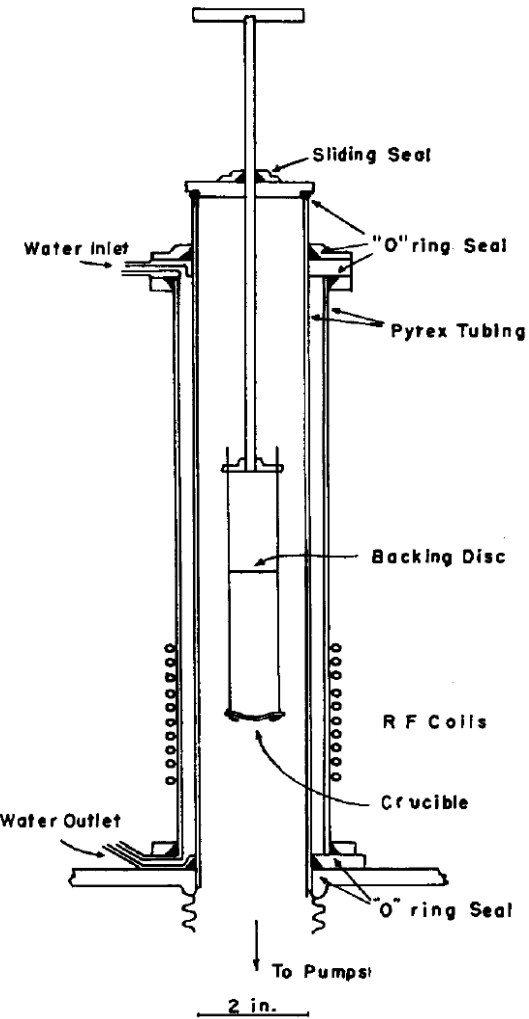
Field amplitude exponentially drops inside conductor
With depth δ increase there is also a phase difference
Lower frequencies are more penetrating $\delta \sim \mu\text{m}$ scale

- For poor conductors heat can be transferred through metal susceptor (coating, crucible)
- Magnetic materials also heat through hysteresis effect (domain wall rotation)

$$P = f \int H d\vec{B}$$

Heating power – existence of hysteresis loop is necessary

Induction Furnace Example



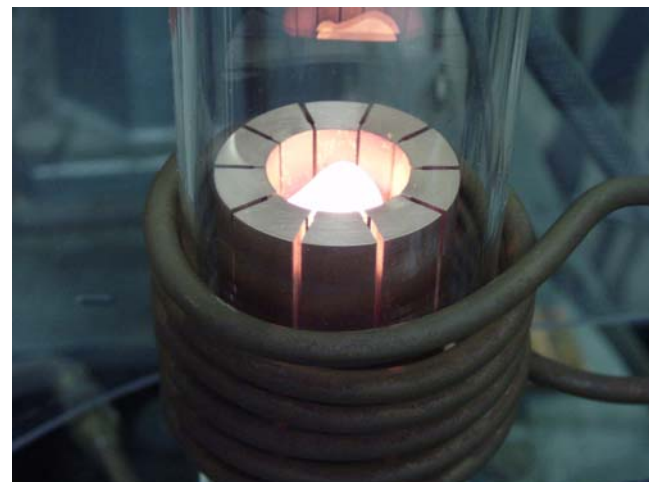
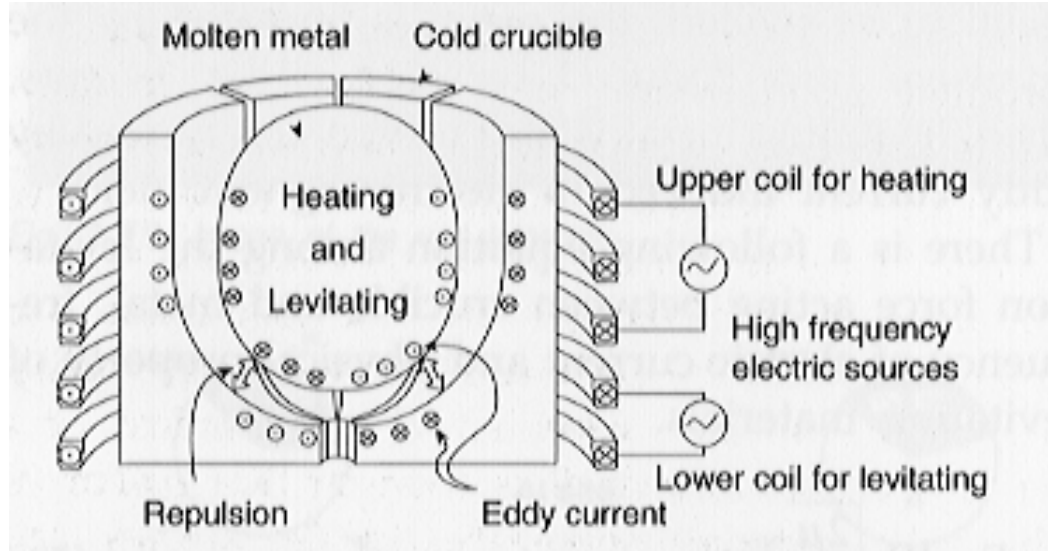
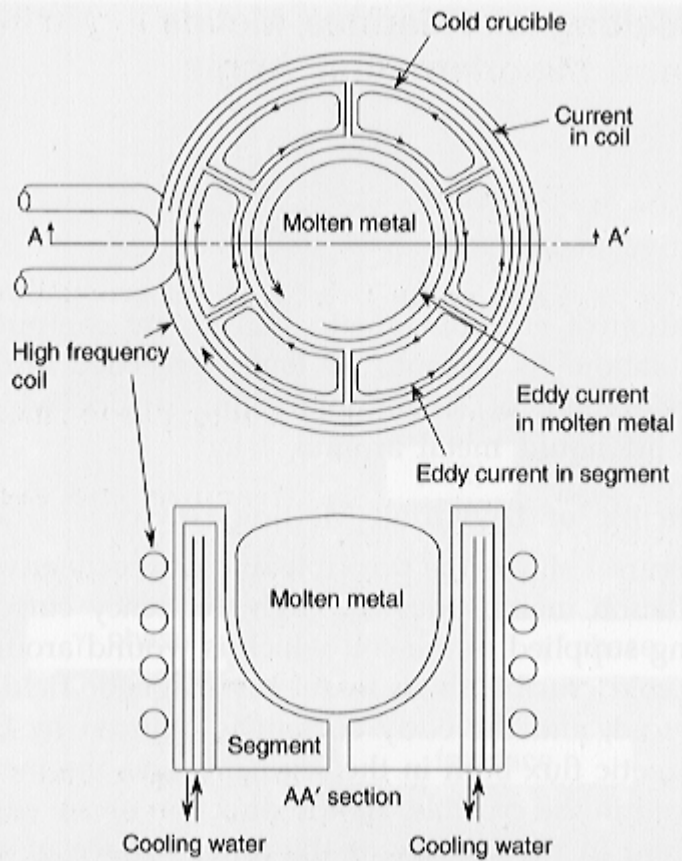
Early apparatus:

The review of scientific instruments 30, 837(1959)

Induction Furnace in the Laboratory

Radio Frequency heating (100-400Khz) using cold copper crucible

Magnetic levitation = kind of crucible-less method



Induction Furnace in the Laboratory



Instrumentation :

- Three two colors infrared pyrometers (500-1000°C ; 900-1700°C, 1000-3000°C)
- High speed shutter Camera
- Hybrid (dry) turbomolecular pumping down to 10^{-8} mbar
- T regulators/programmators
- 50 Kw 100-400Khz RF generator.

Powder Synthesis of Ceramics

Characterized by grain size distribution, shape

Grain size important in mechanical and electronic properties

Balance between Van der Waals attraction and Coulomb repulsion

- *Hot isostatic pressing* (800-3000°C, 7kbar) applies *high pressure* that lowers sintering temperature, powders melt and react, results in dense product.
- Density change with increasing pressure is proportional to porosity

$$\frac{d\rho}{dP} = A \left(1 - \frac{\rho}{\rho_{\max}}\right)$$

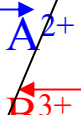
density of fully compacted powder, no pores
density at $P = 0$

$$1 - \frac{\rho}{\rho_{\max}} = \left(1 - \frac{\rho_0}{\rho_{\max}}\right) e^{-\frac{AP}{\rho_{\max}}}$$

- In *sintering* ceramic powder particles merge into a solid at some T so there is a decrease of surface energy. There is diffusion of atoms and molecules along the surfaces or through bulk. Pores are decreasing, smaller in number and density increases.
- Powders have to be dried often to remove moisture. Sometimes are air sensitive.

Solid State Reactions

Often used for precursors, at high T where atoms can diffuse
Two stages: nucleation and growth



Easier for elements with atomic structures and bond lengths within 15%

After nucleation growth controlled by diffusion.

If there is a width of formation ($\text{A}_{1-\delta}\text{B}_{2+\delta}\text{O}_4$) stoichiometry may be different at the interface

Thickness of the product layer is controlled by diffusion, atomic defects, Vacancies \rightarrow defect concentration $\sim 1/\Delta x$

Growth rate :

$$\frac{d(\Delta x)}{dt} = \frac{k}{\Delta x} \longrightarrow (\Delta x)^2 = 2kt$$

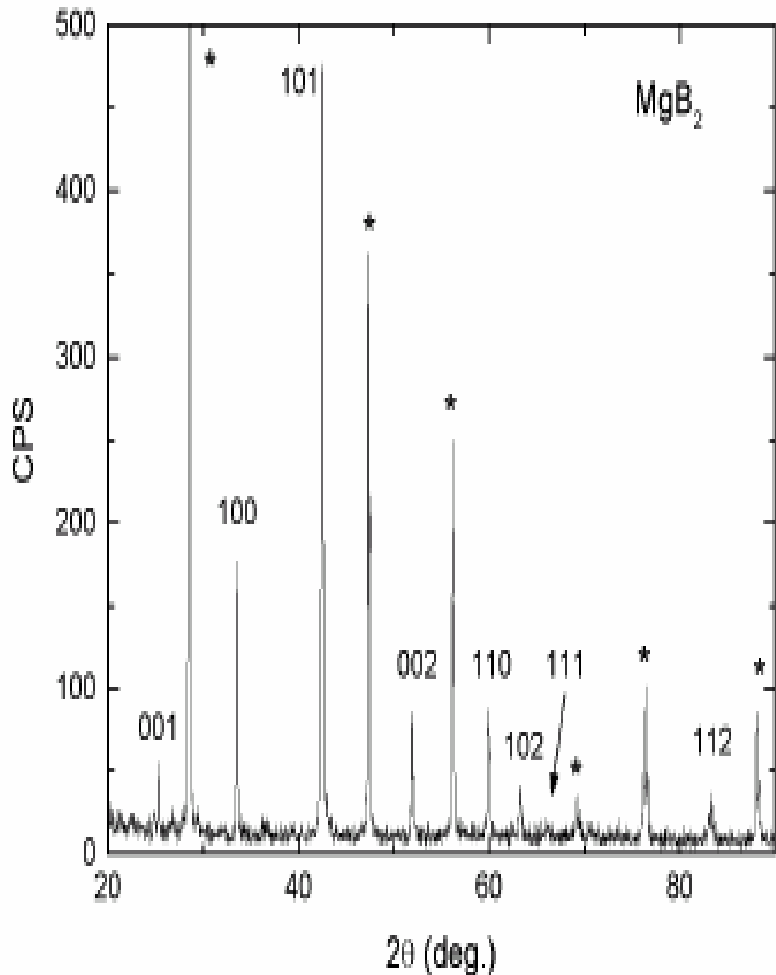
Thickness of the product layer increases parabolically with time

Increasing surface area of powder contact will increase the rate of solid state reaction, will improve homogeneity

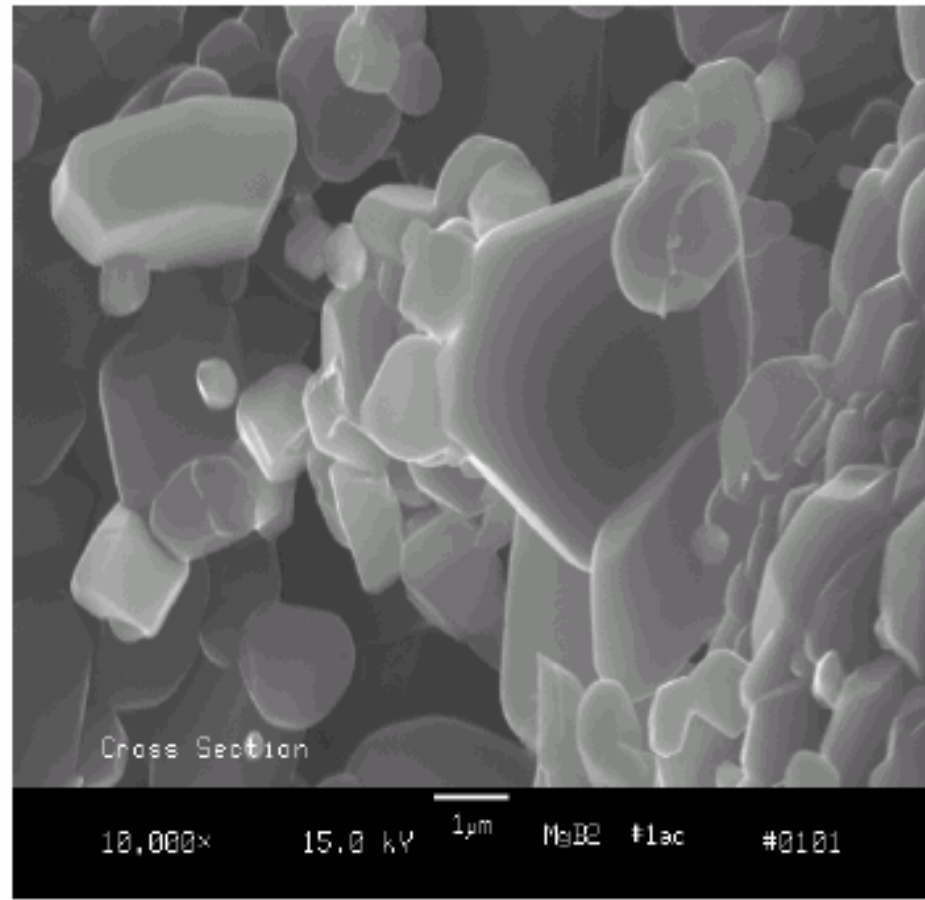
Example: Superconducting powders of MgB_2

Mg in some samples, size MgB_2 (0.5-5) μm . B purity is *crucial*

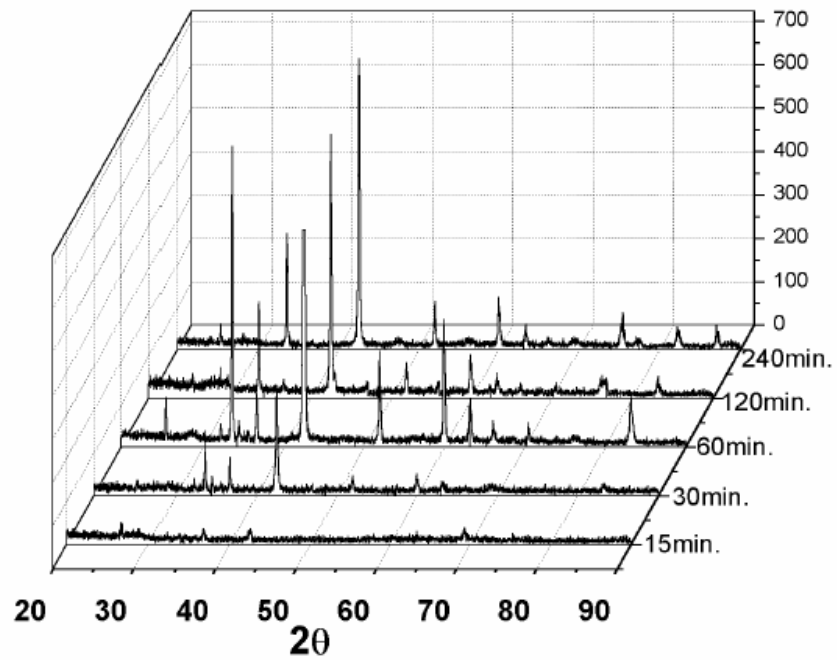
At 950°C Mg vapor is 200Torr \Rightarrow reaction through diffusion of Mg vapor in B



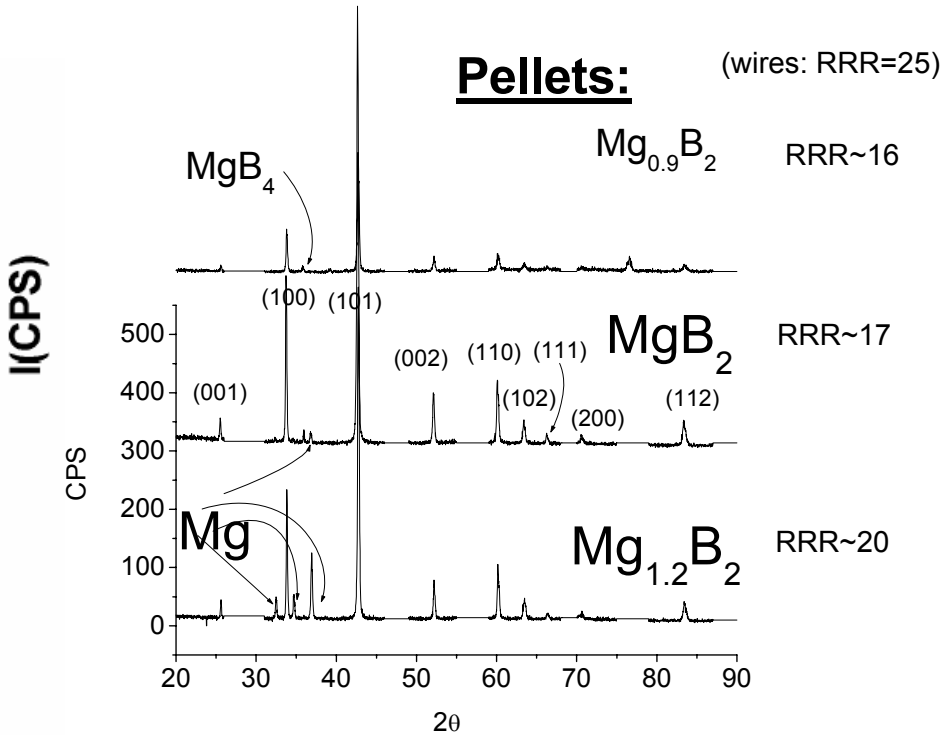
size distribution



Synthesis of MgB_2 powders



Physica C 353, 5 (2001)



Studies of High Temperature Superconductors 38, 1 (2002)

MgB_2 sintering is time dependent

Changes in stoichiometry result in presence of other thermodynamically stable phases
Note how electronic transport properties change

Superconducting wires of MgB_2



Phys. Rev. Lett. 86, 2423 (2001)

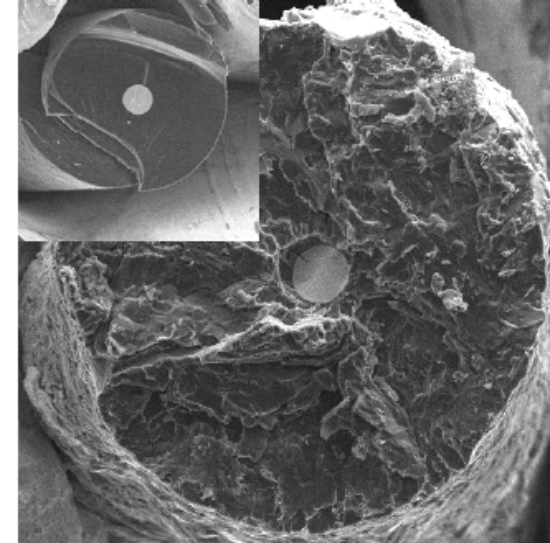


Fig. 6. Electron microscope image of a snap cross section of a $\sim 160 \mu\text{m}$ MgB_2 wire. Inset: Image of the un-reacted $100 \mu\text{m}$ boron filament. Note: in both images a central core of tungsten boride (diameter $\sim 15 \mu\text{m}$) can be clearly seen [7].

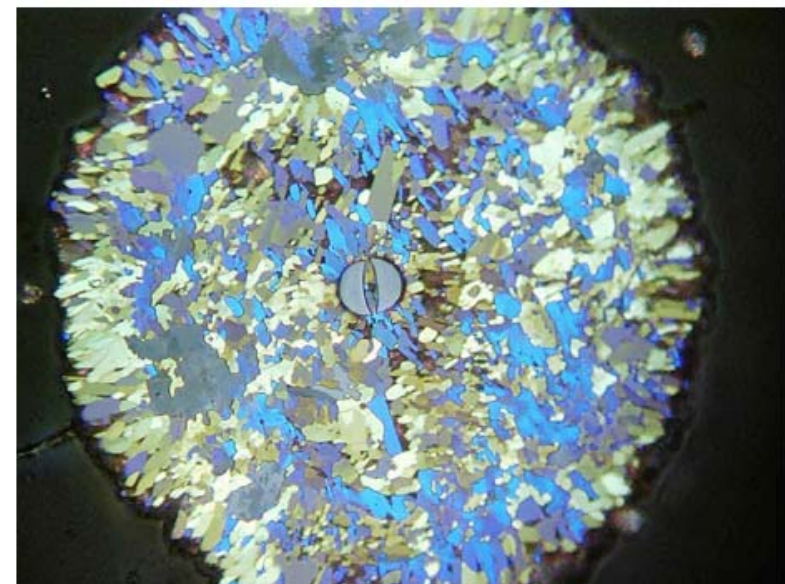
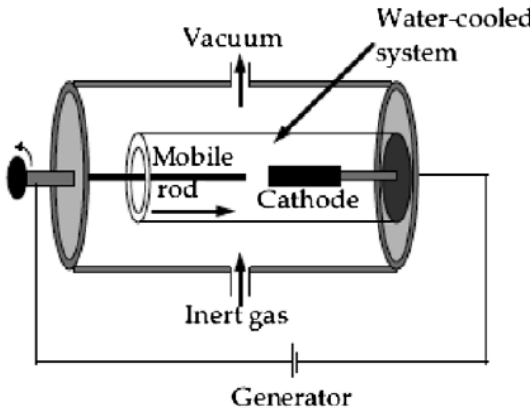


Fig. 7. Optical microscope image (using polarized light) of a polished cross section of $\sim 200 \mu\text{m}$ diameter MgB_2 wire.

Carbon Nanotube Synthesis

- **Planar graphite**: sp^2 bonding, but dangling bonds exist → it is energetically favorable to remove them and form cylindrical shape of a **nanotube** but at the expense of elastic energy which increases by bending.
- There is a minimal radius of the tube is 0.7nm (can't bend the sheet more)
- At very high T of the cathode in carbon arc discharge ($\sim 2500^{\circ}\text{C}$) chemical bonds may lock in this configuration temporarily. Simultaneously C_{60} fullerenes form, exact ratio depends on the pressure in the arc discharge chamber. First discovery made in this way.
- Single and Multi – walled nanotubes are possible, with cylinder distance of 0.34nm , may be controlled by suitably chosen catalysts (Co, Fe...).
- Mechanical properties strength 2X, weight 1/6 of steel
- Metallic or semiconducting



Electric arc discharge between two graphite electrodes under He or Ar atmosphere

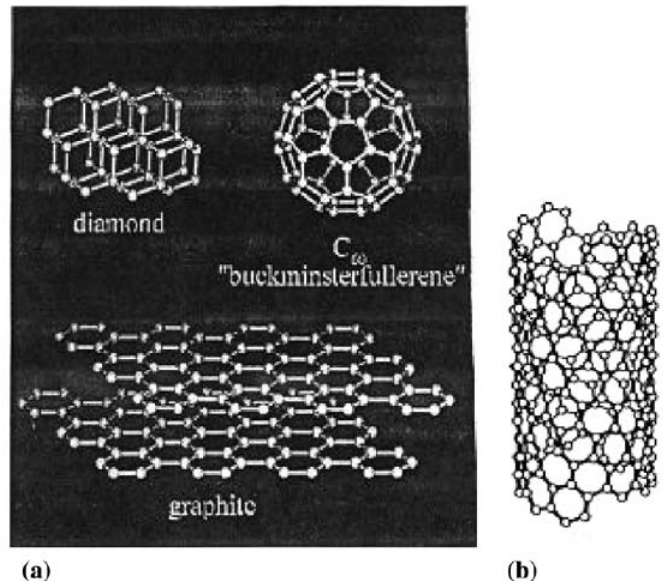


Fig. 4. Structures of (a) diamond, graphite, and fullerene (from R.E. Smalley), (b) a single-wall helical carbon nanotube [3].

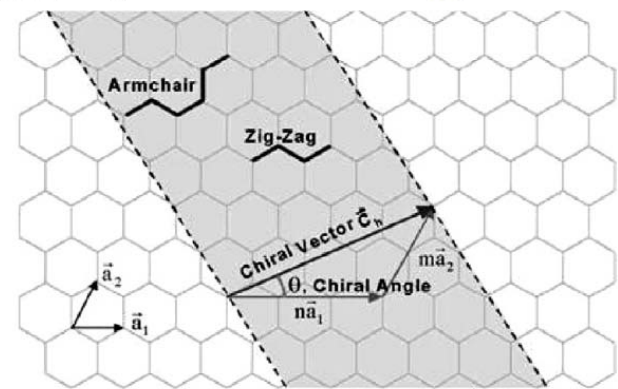
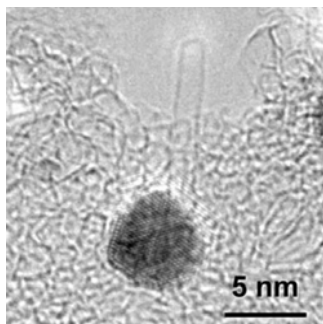


Fig. 6. Schematic diagram showing how a hexagonal sheet of graphite is 'rolled' to form a carbon nanotube [33].

Laser Ablation of Carbon Nanotubes

Phys. Stat. Sol. (b) 11, 3944 (2007), Nanotechnology 19 055605 (2008) – in situ characterization of the process



SWNT is the fastest growing nanotube.
Oversupply of C will result in
additional walls and curving

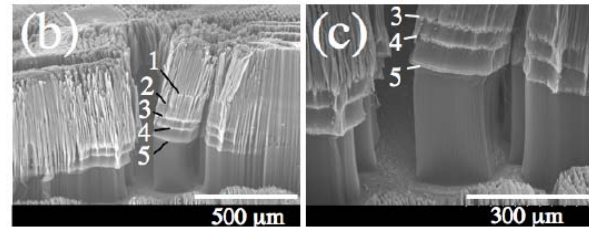
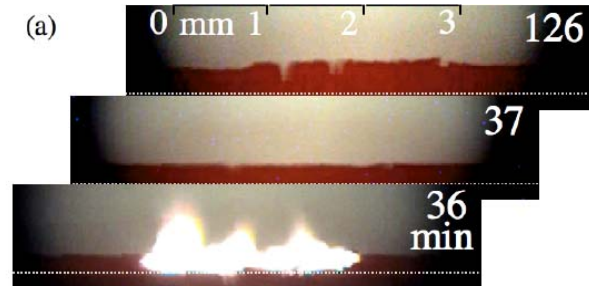
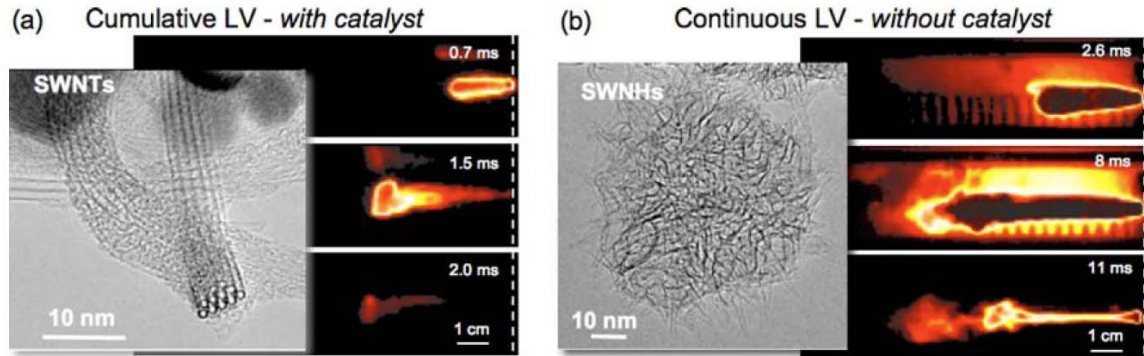
Laser interacts with carbon target containing 1-2 at. % of metal catalyst (Co,Ni)

100 μ s : catalyst and C are atomized, bond breaking

1-2 ms: hot plasma cools, carbon atoms form clusters as hot plasma cools

15 – 20 ms: SWNT seeds are formed

Laser ablation: application of cumulative (~1ms) or single long (~10ms)pulses possible



Vertically aligned nanotube array (VANTA) synthesis

Sequence of frames from 36 to 126 min.

Frame at 36 min. shows laser ablation plume resulting from laser irradiation of VANTA during Growth using several different ablation parameters

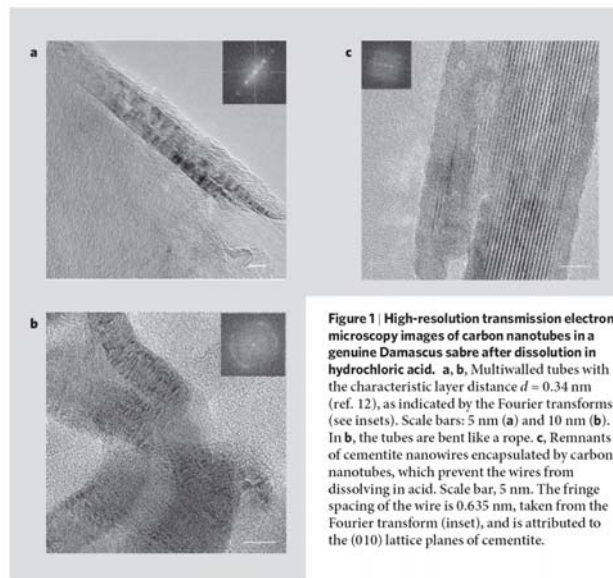
SEM images show aligned nanotube growth – it is possible to adjust parameters and study nanotube growth and mechanisms of orientation.

Bulk Synthesis in CMMP

Applications of Carbon Nanotubes

MATERIALS

Carbon nanotubes in an ancient Damascus sabre



The steel of Damascus blades, which were first encountered by the Crusaders when fighting against Muslims, had features not found in European steels — a characteristic wavy banding pattern known as damask, extraordinary mechanical properties, and an exceptionally sharp cutting edge. Here we use high-resolution transmission electron microscopy to examine a sample of Damascus sabre steel from the seventeenth century and find that it contains carbon nanotubes as well as cementite nanowires. This microstructure may offer insight into the beautiful banding pattern of the ultrahigh-carbon steel created from an ancient recipe that was lost long ago.

It is believed that Damascus blades were forged directly from small cakes of steel (named 'wootz') produced in ancient India. A sophisticated thermomechanical treatment of forging and annealing was applied to these cakes to refine the steel to its exceptional quality. However, European bladesmiths were unable to replicate the process, and its secret was lost at about the end of the eighteenth century. It was unclear how medieval blacksmiths would have overcome the inherent brittleness of the plates of cementite (Fe_3C , a mineral known as cohenite) that form in steel with a carbon content of 1–2 wt%, as well as how the steel's characteristic banding could have arisen from

APPLIED PHYSICS LETTERS 89, 123127 (2006)

Ancient



Energy absorption capacity of carbon nanotubes under ballistic impact

Kausala Mylvaganam^{a)} and L. C. Zhang^{b)}

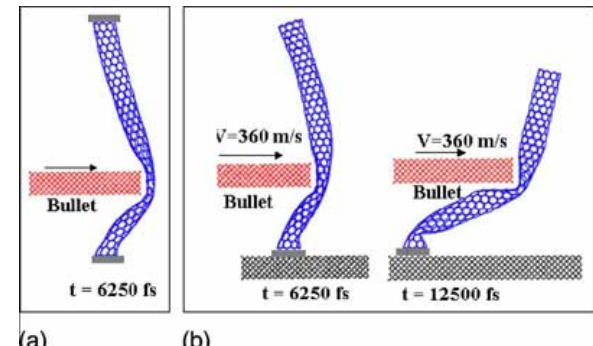
Centre for Advanced Materials Technology, The University of Sydney, New South Wales 2006, Australia

(Received 28 April 2006; accepted 28 July 2006; published online 22 September 2006)

Carbon nanotubes have great potential applications in making ballistic-resistance materials. This letter analyzes the impact of a bullet on nanotubes of different radii in two extreme cases. For a nanotube with one end fixed, the maximum nanotube enduring bullet speed increases and the energy absorption efficiency decreases with the increase in relative heights at which the bullet strikes; these values are independent of the nanotube radii when the bullet hits at a particular relative height. For a nanotube with both ends fixed, the energy absorption efficiency reaches minimum when the bullet strikes around a relative height of 0.5. © 2006 American Institute of Physics.

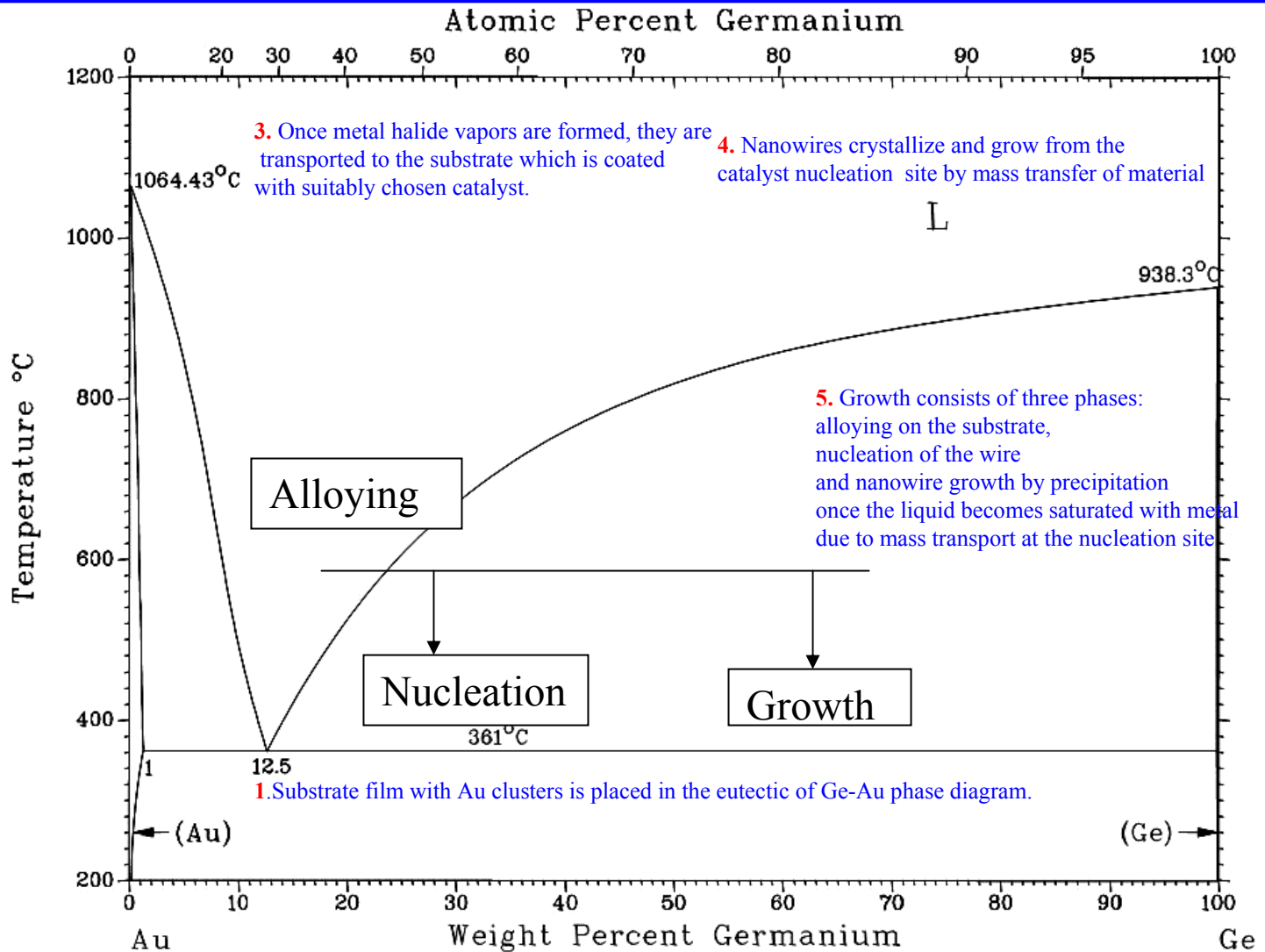
[DOI: [10.1063/1.2356325](https://doi.org/10.1063/1.2356325)]

And Modern



Nanowire Synthesis

VLS growth mechanism on the example of the growth of Ge nanowires at Au catalyst sites



Nanowire Synthesis

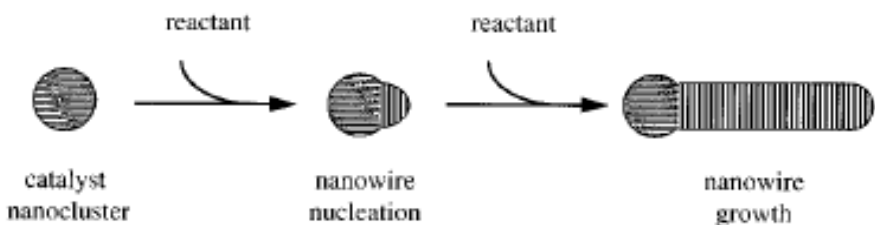


FIGURE 1. Schematic diagram illustrating the catalytic synthesis of nanowires. Reactant material, which is preferentially absorbed on the catalyst cluster, is added to the growing nanowire at the catalyst–nanowire interface.

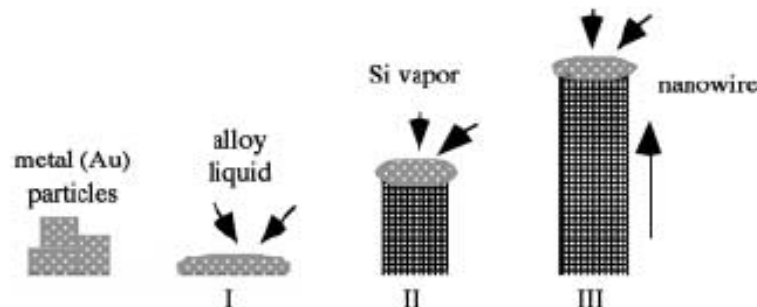
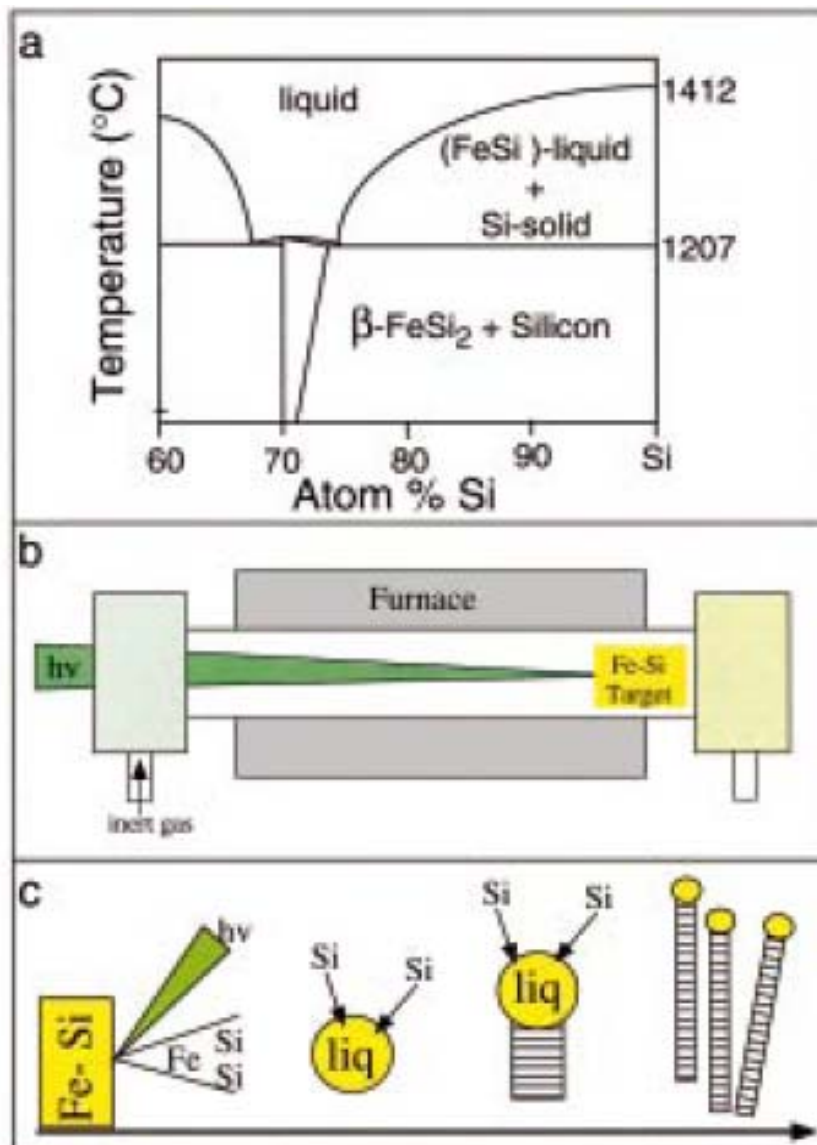
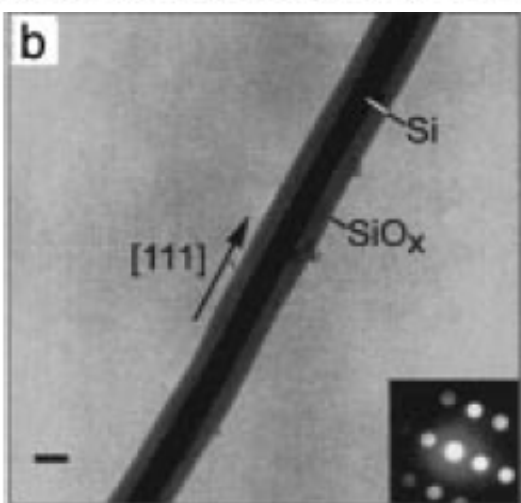
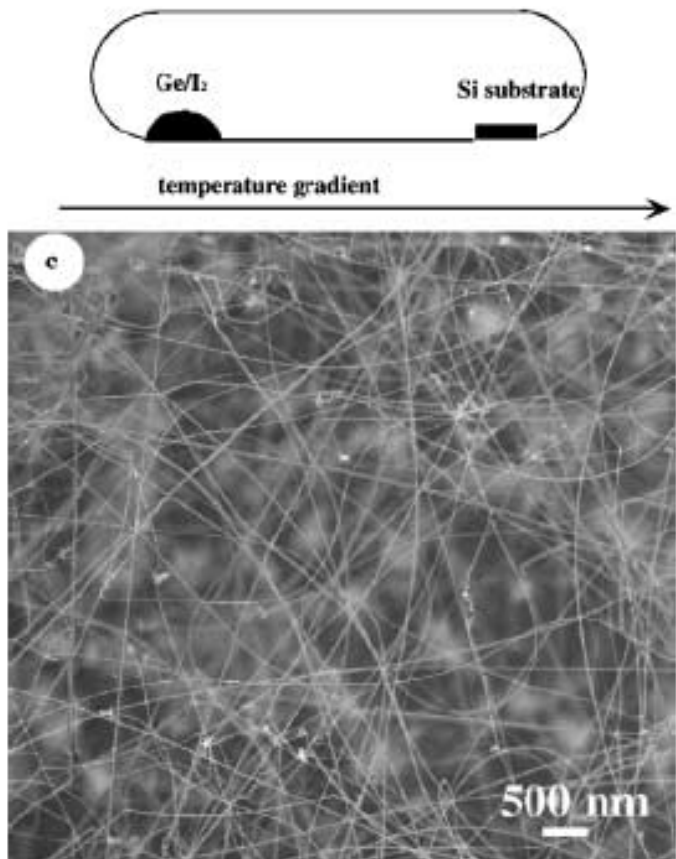
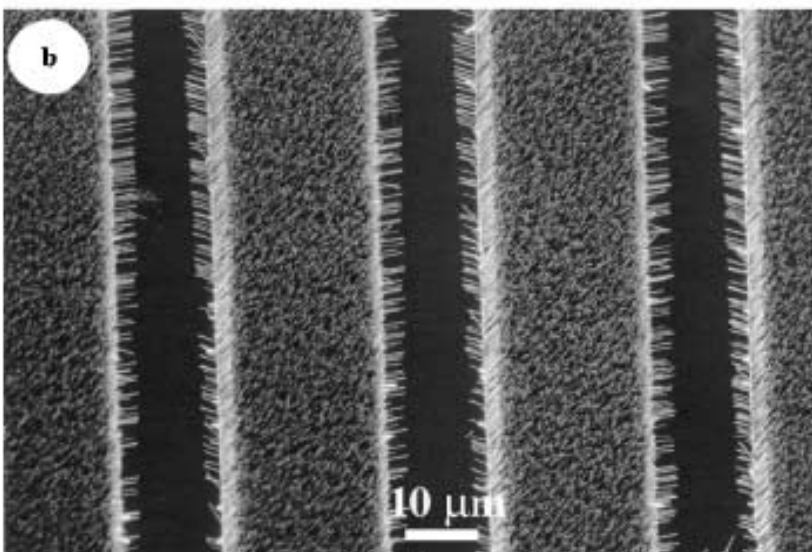
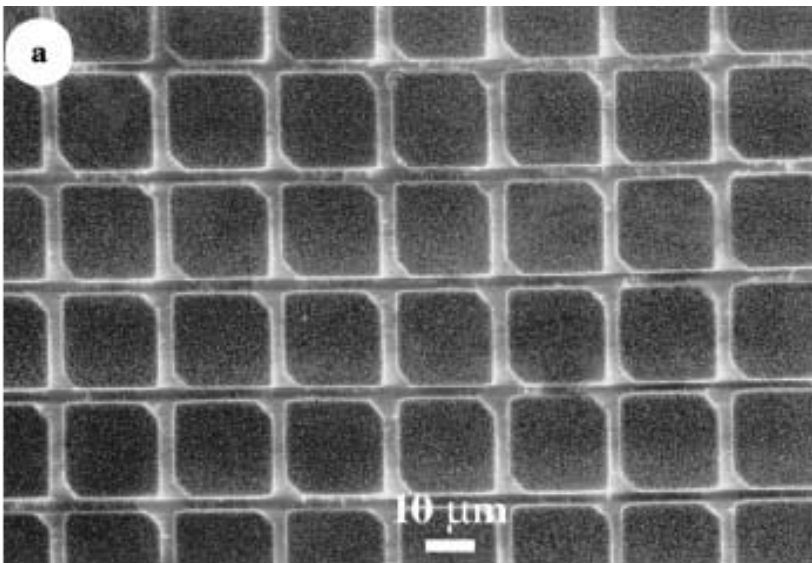


Figure 1. Schematic illustration of vapor–liquid–solid nanowire growth mechanism including three stages: I) alloying, II) nucleation, and III) axial growth.





Disordered vs. ordered nanowire growth



Superconducting MgB₂ nanowires

nanowire as model system.^[7,8] In addition, MgB₂ nanowires can also serve as the building blocks in superconducting nanodevices such as low dissipation interconnects. Here we report the first preparation of MgB₂ nanowires by a two-step vapor transport and reaction process. In the first step, boron nanowires are prepared by chemical vapor transportation reaction. These boron nanowires are then transformed into MgB₂ nanowires by reacting with Mg vapor. The as-prepared nanowires have diameters of 50–400 nm and length up to tens of micrometers.

The preparation of boron nanowires was carried out in a sealed quartz tube. 20–35 mg boron, 0.5–1 mg I₂, and 0.1–0.5 mg Si were put in one end of the tube (diameter 0.5 inch, length 3 inch, 1 inch ≈ 2.5 cm) and an MgO substrate was put in the other end of the tube. The MgO substrate was coated with 5 nm Au thin film using Desktop II Denton sputtering system. The tube was evacuated to 100 mtorr, sealed and then heated to 1000–1100 °C. A temperature gradient of 100 °C was kept between the source materials and the MgO substrate. At the hot zone, boron reacts with I₂ and forms BI₃ vapor. At low temperature zone, BI₃ vapor decomposes, as a result, boron deposits onto the MgO substrate. After 30 min of transport reaction, the furnace is cooled down to room temperature. Fluffy black products were observed on MgO substrate.

